Enhanced Modified Magnetite Bentonite-CaO/$FeCl_3$ from Solid Waste for Highly Efficient Methylene Blue Removal

Yudha Gusti Wibowo[1,2,3*], Hana Safitri[1], Kholivia Cahyani[1,2], Arif Rohman[4], Sudibyo[5], Ahmad Tawfiequrahman Yuliansyah[2], Himawan Tri Bayu Murti Petrus[2], Setyo Budi Kurniawan[6], Bimastyaji Surya Ramadan[7], Anis Tatik Maryani[8], Hutwan Syarifuddin[8]

[1]Sustainable Mining and Environmental Research Group, Department of Mining Engineering, Institut Teknologi Sumatera, Lampung-35365, Indonesia

[2]Sustainable Mineral Processing Engineering, Department of Chemical Engineering, Universitas Gadjah Mada, Yogyakarta, Indonesia

[3]Center for Green and Sustainable Materials, Institut Teknologi Sumatera, Lampung-35365, Indonesia

[4]Department of Geomatic Engineering, Institut Teknologi Sumatera, Lampung-35365, Indonesia

[5]Research Center for Mining Technology, National Research, and Innovation Agency, Lampung-35361, Indonesia

[6]Department of Chemical and Process Engineering, Faculty of Engineering and Built Environment, Universiti Kebangsaan Malaysia, UKM, Bangi, Selangor 43600, Malaysia

[7]Department of Environmental Engineering, Universitas Diponegoro, Semarang, Indonesia

[8]Postgraduate Program of Environmental Science, Universitas Jambi, Jambi, Indonesia

*Correspondence email: yudha.wibowo@ta.itera.ac.id; yudhagustiwibowo@mail.ugm.ac.id

ACCEPTED MANUSCRIPT

Abstract

This study focuses on the development and evaluation of novel materials bentonite-CaO, magnetite bentonite-$FeCl_3$, and magnetite bentonite-CaO/$FeCl_3$ as potent adsorbents for the removal of methylene blue dyes from aqueous solutions. Batch adsorption test was conducted with variations of contact times and dye concentrations. The maximum sorption capacity reached 39 mg/g with Langmuir isotherm model (R^2=0.999) following the pseudo second-order kinetic model. The materials exhibited exceptional effectiveness, achieving a remarkable 99% reduction in methylene blue concentration within an astonishingly short 10-minute duration. Additionally, this study provides valuable insights into the potential applications of these modified adsorbents in

environmental remediation, accompanied by practical recommendations for their utilization in various scenarios.

Keywords: Adsorption; Bentonite-CaO; Bentonite-$FeCl_3$; Bentonite-CaO/$FeCl_3$; Dyes removal; Methylene Blue

1. Introduction

The United Nations World Water Development Report estimated that approximately four million individuals globally are confronted with freshwater scarcity as a consequence of climate change (UNESCO, 2020). This data predicted an increase rapidly for 30 years ago up to more than 10 billion people. According to another published paper, a recent study projects that by 2050, 6 billion individuals will be afflicted by the scarcity of pure water. Presently, this predicament is a significant concern in a world inhabited by 7.7 billion individuals (Boretti and Rosa, 2019). According to a separate estimate by the Food and Agriculture Organization (FAO) of the United Nations, around one-sixth of the world's population, or approximately 1.2 billion individuals, reside in agricultural regions with severe water constraints or scarcity. This accounts for 3.2 billion of the world's population residing in regions with high to extremely high water shortages or scarcity (Food and Agriculture Organization of the United Nations, 2020).

Therefore, it is essential to develop various strategies to treat wastewater, particularly from sewage plants, as a means to address these pressing water scarcity issues. Additionally, the widespread environmental pollution caused by dyestuff has become a major global concern for maintaining a healthy environment. Dye pollution poses hazardous consequences for all living organisms and can disrupt photosynthesis and food chains, depending on the ecosystem (Alsukaibi, 2022; Al-Tohamy et al., 2022; Awad et al., 2023; Mittal et al., 2009). Dyes are known to be very dangerous for environments and human health, even in a recent published paper reported that dyes are highly toxic, carcinogenic, mutagenic and resistant to degradation (He et al., 2018a; Kishor et al., 2021; Shanker et al., 2017; Siddiqui et al., 2010). Regrettably, these dyes are widely utilized across a range of industries such as textiles, cosmetics, food, pharmaceuticals, paper, and leather, resulting in a significant global production of dyes with 10,000 different dyes (Farhan Hanafi and Sapawe, 2019; Oladoye et al., 2022; Saini et al., 2018; Samsami et al., 2020; Tkaczyk et al., 2020; Tomar and Dahiya,

ACCEPTED MANUSCRIPT

2022). Consequently, the discharge of these dyes into ecosystems leads to undesirable environmental burdens.

Several dyes such as methylene blue, Congo red and methyl orange that's common dyes can be found in the industrial activities. From the three dyes that commonly found, methylene blue is one of most common substance that used in industry. This dye is a dangerous for the ecosystem even in low concentration. Several studies were reported their effort to solve this problem, but the problem of dyes still exist. A recent study reported that the phytoremediation for removal methylene blue and Congo red using *Lemna minor* was successfully degradation, but it is need long of times (up to 24 days) (Wibowo et al., 2023b) and still not removal effective of all dyes. The same result showed in other method including bioremediation with bacteria (Upendar et al., 2017), coagulation/flocculation (Lau et al., 2015) and filtration (Doke and Yadav, 2014).

Adsorption has been widely recognized as one of the most effective, efficient, and cost-efficient methods for removing dyes from wastewater (Asuha et al., 2020; Bestani et al., 2008; El-Halwany, 2010). Bentonite, a naturally occurring material, has shown promise in adsorbing dyes onto its pores and surface area. Previous studies have demonstrated that natural bentonite successfully reduced methylene blue by 80% (Islam and Mostafa, 2022). To further enhance the adsorption performance of bentonite, researchers have explored modifications, leading to the development of high-performance adsorbents for dye removal (Bergaoui et al., 2018; De Castro et al., 2018a; Gupta et al., 2015a). Despite noteworthy progress in research and development, the challenge of dye pollution persists, mainly attributed to the high production costs of advanced adsorbent materials. In this study, we have addressed this challenge by creating a high-performance modified magnetite bentonite using waste from crab shells. This innovative approach aims to overcome cost barriers and improve the efficiency of dye removal.

Importantly, to the best of our knowledge, no data on the application of modified magnetite bentonite-CaO/$FeCl_3$ for methylene blue removal have been reported. Therefore, this study is significant in filling this research gap and contributing to the field of adsorption for methylene blue removal, using a low-cost and eco-friendly modified adsorbent. By exploring the potential of modified magnetite bentonite-CaO/$FeCl_3$, this study provides valuable insights into the development of cost-effective and sustainable solutions for tackling dye pollution in wastewater. The use of waste materials, such as crab shells, not only addresses environmental concerns but

ACCEPTED MANUSCRIPT

also demonstrates the possibility of transforming waste into a valuable resource for water treatment applications. Thus, this study represents a crucial step forward in the field of adsorption for dye removal, specifically methylene blue, by introducing a novel and economically viable adsorbent. The results obtained in this research contribute to the expansion of knowledge in the field and open avenues for further exploration of low-cost and efficient adsorption materials for wastewater treatment applications. Additionally, this work has the potential to make a positive impact on environmental preservation and water quality improvement.

2. Materials and Method

2.1 Raw Materials, Dyes and Reagent

Raw materials in this study are bentonite, and crab shell waste. Bentonite was bought from the online store in Indonesia and crab shell waste was collected from the seafood restaurant around Lampung Province, Indonesia. $FeCl_3$ and methylene blue ($C_{16}H_{18}ClN_3S$) in this study were obtained from Merck, Germany. The distilled water that was used in this study produced by Laboratory of Chemical Science, Institut Teknologi Sumatera. To simulate wastewater, 1000 ppm of methylene blue was used as a stock solution.

2.2 Preparation Materials

Bentonite was crushed into small sizes and agitated with 200 mesh shaving shakers. Then, bentonite was dried by Universal Drying Oven LabTech LDO 100E, Korea at 150 °C for 3 hours. After dried, the sample was pyrolyzed at 600 °C for 3 hours. Crab shell waste was also crushed and agitated with 200 mesh of shaving shaker. Then the small particle of crab shell was calcinated using Muffle Furnace at 800 °C for 2 hours. A 1 M of magnetite solution ($FeCl_3.6H_2O$) was used in this study. This study used three variations of modified bentonite including magnetite bentonite (Bentonite-$FeCl_3$), bentonite-CaO and Bentonite-CaO/$FeCl_3$. Magnetite bentonite was created by adding Iron(III) Chloride hexahydrate 1 M with ratio of 1:1. The second variation of bentonite-CaO was created by adding bentonite and CaO also with ratio 1:1, and the last variation of bentonite-CaO/FeCl3 was created by adding 1:1 ratio of first variation of bentonite-FeCl3 and CaO. Prepared materials will be characterized by X-Ray Florescence for characteristic the elements of samples. The illustration in preparation of materials can be seen in **Figure 1**.

ACCEPTED MANUSCRIPT

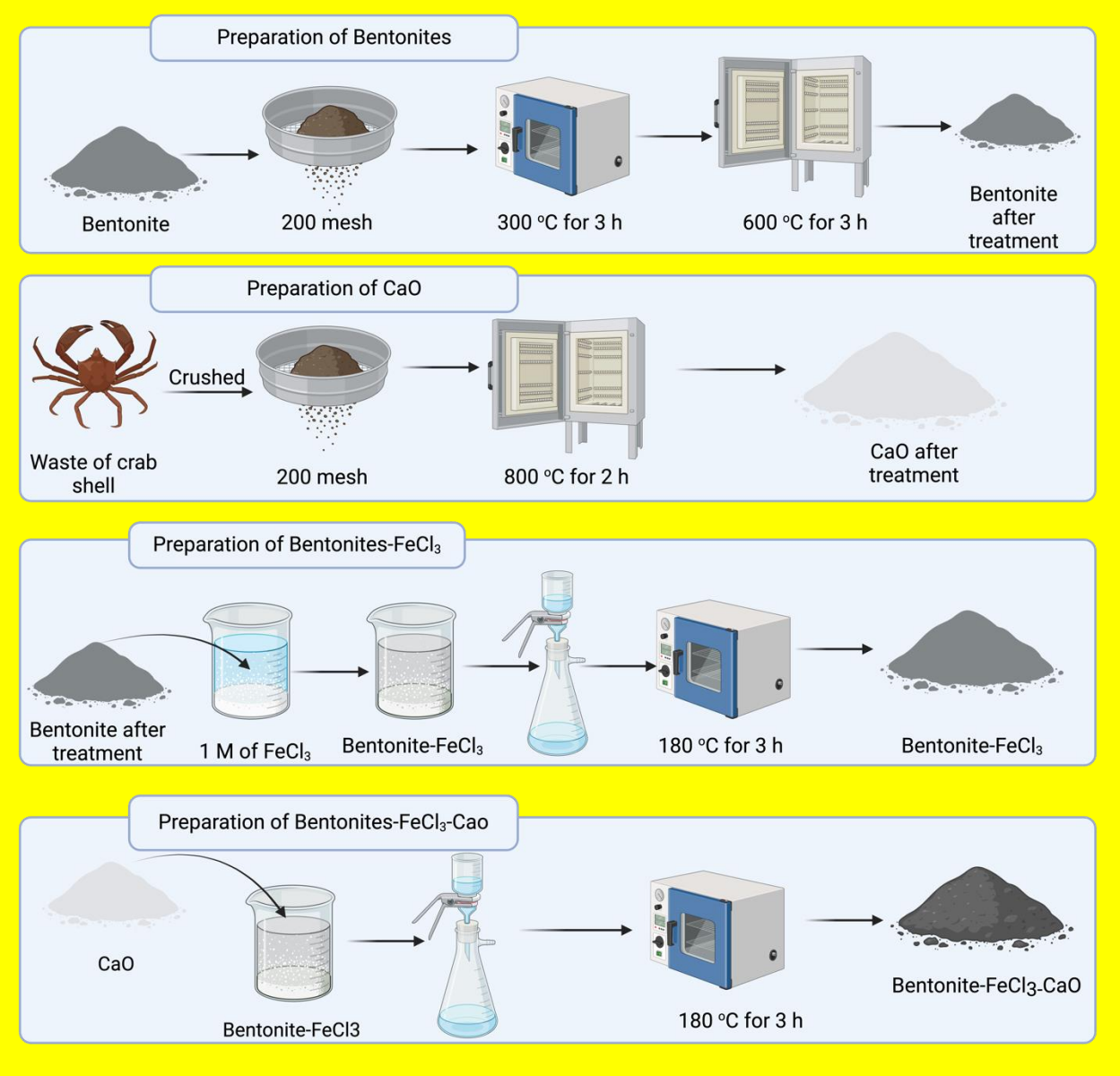

Figure 1. Materials preparation

2.3 Materials Characteristic

All materials will undergo X-Ray Fluorescence (XRF) PANAnalytical Minipal 4 to determine the concentration of magnetite in the samples. Additionally, the presence of CaO derived from crab shells will be identified for future research direction, considering its potential for neutralizing acidic conditions in polluted water. The subsequent characterization will involve Fourier Transform Infrared (FTIR Bruker, Germany) analysis, critical step to identify functional groups

resulting from the addition of CaO and $FeCl_3$, aimed at creating a novel modified bentonite-CaO/$FeCl_3$ composite.

XRF analysis will provide valuable data on the magnetite content within the materials, which is essential for understanding their magnetic properties and potential applications in various fields. Identification of CaO derived from crab shells opens possibilities for future research focused on its role in neutralizing acid-contaminated water. This aspect is particularly significant as it can pave the way for environmentally friendly remediation strategies. The FTIR analysis will play a crucial role in characterizing the modified bentonite-CaO/$FeCl_3$ composite. By identifying the functional groups present, this analysis will provide insights into the chemical interactions between the materials, helping to optimize their composition and enhance their potential for specific applications.

2.4 Performance Test

Performance test of a novel materials bentonite-CaO, bentonite-$FeCl_3$ and bentonite-CaO/$FeCl_3$ were tested in two variation including time contact effect and concentration of dyes effect. The contact times that were used in this study are 0, 10, 20, 40, 60, 100, 200, 300 dan 400 minutes. Besides, the effect of concentration will be measured by variation of methylene blue concentration including 20, 40, 60, 80 and 100 ppm. In contact time effect, 1 gr of materials will be added into 200 ppm of artificial methylene blue solution at 200 rpm. Furthermore, the concentration effect tested by adding 0.5 gr of materials for 10 minutes at 200 rpm. Then, all of methylene blue solution measured by UV-VIS (Spectrophotometer UV Vis, Thermo) with wavelength 664 nm. Percent removal and sorption capacity of materials measured by Eq. 1 and Eq. 2 (Wibowo et al., 2022).

$$Sorption\ capacity = \frac{V(C_0 - C_e)}{W} \qquad \text{Equation 1}$$

$$Removal\ percentage = \frac{C_0 - C_e}{C_0} x100\% \qquad \text{Equation 2}$$

2.4 Isotherm Models

Five models will be utilized to evaluate the sample's isotherm model: Freundlich, Langmuir, Temkin, Brunauer–Emmett–Teller (BET), and Dubinin–Radushkevich. One of the critical

ACCEPTED MANUSCRIPT

parameters in determining the adsorption mechanism between a substance and an adsorbate is the isotherm model. The Freundlich model of isotherm can be determined using Equation (3).

$$q_e = \frac{q_m k_a c_e}{1 + k_a c_e} \quad \text{Equation 3}$$

Eq. 3 also could be written as Eq. 4

$$\frac{C_e}{q_e} = \frac{C_e}{q_m} + \frac{1}{k_a q_m} \quad \text{Equation 4}$$

In the given context, q_e (mg g^{-1}) denotes the quantity of adsorbed contaminant per unit mass of adsorbent, Ce (mg L^{-1}) represents the equilibrium concentration of hard water, q_m signifies the material's adsorption capacity, and K_a(L mg^{-1}) is a constant associated with the affinity of binding sites [30]. The evaluation of the Langmuir model's suitability could be conducted by calculating the intensity of adsorption (R_L), which is given in Equation 5.

$$R_L = \frac{1}{1 + k_a c_m} \quad \text{Equation 5}$$

Where c_m is the initial concentration of hard water.

The Freundlich model suggested that surface adsorption processes on adsorbents are heterogeneous. The calculation for the Freundlich model is given in Equation 6.

$$q_e = K_f C_e^{1/nF} \quad \text{Equation 6}$$

Eq. 6 also could be written as Eq. 7

$$logq_e = logK_F + \frac{1}{n} logC_e \quad \text{Equation 7}$$

Where K_F (mg m^{-1}) (L g^{-1}) and 1/n are sorption capacities and adsorption intensity, respectively.

The Temkin isotherm, which constitutes the third model, incorporates a factor that is directly associated with the interaction between the adsorbent and the adsorbate. This model operates under the assumption that the adsorption energy or heat of every molecule in the layer will diminish linearly as coverage increases, as a result of the adsorbent-adsorbate interaction, by disregarding

ACCEPTED MANUSCRIPT

extremely low or high concentration values. Equation 8 presents the equation form of the Temkin adsorption model.

$$Q_e = \frac{RT}{bt}\ ln\ C_e \qquad \text{Equation 8}$$

The linear form of Equation 8 with the bonding energy can be written as follows:

$$Q_e = B_T \ln A_T + B_T \ln C_T \qquad \text{Equation 9}$$

Qe = amount of substance adsorbed at equilibrium (mg g^{-1}) Ce = adsorbate concentration at equilibrium (mg L^{-1}) BT = (RT) / bt with bt = heat constant AT = equilibrium bonding constant (L min^{-1}).

The BET isotherm, an extension of the Langmuir isotherm model, is a sophisticated framework designed to describe multilayer adsorption. The evaporation (desorption) rate from the surface occupied by a single adsorbate molecule is equivalent to the condensation (adsorption) rate from the vacant surface of the adsorbent. The BET adsorption model can be expressed in the following equation form (Eq. 10).

Equation 10

$$Q_e = \frac{Q_o K \frac{C_e}{C_o}}{\left(1 - \frac{C_e}{C_o}\right)\left[1 + 9K - 1\frac{C_e}{C_o}\right)}$$

Qe = number of ions adsorbed K = adsorption equilibrium constant Qo = maximum adsorbent uptake capacity for the adsorbate Ce = final concentration Co = initial concentration.

The Dubinin-Radushkevich isotherm is a model expressed by a semi-empirical equation that predicts the adsorption process follows a mechanism of pore filling. The underlying presumption of this model is that physical adsorption processes are characterized by multilayer adsorption facilitated by van der Waals forces. The linear representation of this adsorption model is denoted by equation 11.

ACCEPTED MANUSCRIPT

$$Ln\ q_e = \ln qs - K_{ad}\ \times \varepsilon^2 \qquad \text{Equation 11}$$

In the context, qe, qs, and Kad represent the amount of adsorbate on the adsorbent at equilibrium conditions (mg g^{-1}), the theoretical monolayer saturation capacity (mg g^{-1}), and the equilibrium constant, respectively. Ɛ is the Dubinin-Radushkevich isotherm constant. The value of Ɛ can be determined using Equation 12

$$\varepsilon\ = RT \ln(1 + \frac{1}{C_e}) \qquad \text{Equation 12}$$

Meanwhile, the energy value used to determine the nature of adsorption, which is the average free energy per mole of adsorbate, can be calculated using Equation 13.

$$R = \frac{1}{\sqrt{2K_{ad}}} \qquad \text{Equation 13}$$

2.5 Kinetic Models

Adsorption kinetics, which denotes the rate at which the adsorbent absorbs the adsorbate, is an essential component of the adsorption process. An additional factor utilized in the determination of adsorption duration is adsorption kinetics. Adsorption kinetic models that are frequently employed in the context of liquid-phase adsorption are pseudo-first order and pseudo-second order. To implement the pseudo-first-order kinetic model, ln(qe-qt) is plotted against t (time), whereas to implement the pseudo-second-order kinetic model, t/qt is plotted against t (time). The kinetics model utilized in this investigation can be computed using Equations 14 to 16.

$$C_A = C_{A0} - kt \qquad \text{Equation 14}$$

$$\ln(qe - qt) = \ln qe - K_{ft} \qquad \text{Equation 15}$$

$$\frac{1}{qt} = \frac{1}{K_2 q_{e^2}} = \frac{1}{qe}t \qquad \text{Equation 16}$$

Where qe = adsorption capacity at equilibrium (mmol g^{-1}), qt = adsorption capacity at time t (mmol g^{-1}), kf = pseudo-first-order rate constant ($minute^{-1}$), ks = pseudo-second-order rate constant (g

ACCEPTED MANUSCRIPT

mmol $^{-1}$ minute^{-1}), C_A = concentration of A at time t, C_{A0} = initial concentration of A, t = time (minutes).

2.6 Thermodynamic Analysis

The following equations were utilized to estimate the thermodynamic parameters (ΔG°, ΔH°, and ΔS°): where R represents the gas constant (8.314 J·mol^{-1} K^{-1}), T denotes the temperature in Kelvin (K), Kd signifies the distribution coefficient, qe signifies the phenol equilibrium concentration on the adsorbent (mg L^{-1}), and Ce signifies the phenol equilibrium concentration in the solution (mg L^{-1}). The calculation of free energy change (ΔG°) is feasible via equation 17, while the determination of enthalpy change (ΔH°) and entropy change (ΔS°) are both possible via the Van't Hoff equation 18 and equation 19, respectively. (Mojoudi et al., 2019).

$$\Delta G^o = -RT \ln K_d \qquad \text{Equation 17}$$

$$K_d = {}^{Q_e}/_{C_e} \qquad \text{Equation 18}$$

$$\Delta G^o = \Delta H^o - T\Delta S^o \qquad \text{Equation 19}$$

3. Result and Discussion

3.1 Characteristic Materials

Characterization using Fourier Transform Infrared (FTIR) spectroscopy was conducted to compare the functional groups present in three types of adsorbents: BC, BF, and BFC. FTIR spectroscopy allows for the analysis of molecular vibrations, providing valuable insights into the adsorption capabilities of these materials. The obtained spectra revealed several significant functional groups present in the adsorbents; Figure 2 showed the functional groups of each material. BC showed a broad peak at 3625.69 cm^{-1} indicates the presence of hydroxyl groups (-OH), originating from water and surface hydroxyls on the bentonite, this study is relevant to the previous study that used natural bentonite for the removal of lead ions (Yang et al., 2022). Peaks observed at 1633.72 cm^{-1} and 1759.06 cm^{-1} are attributed to the bending and stretching vibrations of water molecules, respectively. The peak at 1006.56 cm^{-1} suggests the presence of Si-O-Si stretching vibrations, characteristic of the bentonite structure. Additionally, a broad peak in the range of 941.43 cm^{-1} to

ACCEPTED MANUSCRIPT

1034.05 cm^{-1} indicates the presence of carbonate ions (CO_3^{2-}) from $CaCO_3$, possibly due to the presence of CaO in the material.

In addition, BF informed several modified peaks such as peaks observed at 3377.83 cm^{-1} and 3340.48 cm^{-1} indicate the presence of hydroxyl groups (-OH) and water molecules, similar to BC. The peak at 1623.98 cm^{-1} could indicate the presence of water bending vibrations. The peak at 787.71 cm^{-1} might correspond to the Fe-OH bending vibration, indicating the interaction between $FeCl_3$ and the bentonite. Besides, the last modification known as BFC informed the several peaks including the presence of broad peaks at 3381.33 cm^{-1} and 3340.48 cm^{-1} indicates the presence of hydroxyl groups (-OH) and water molecules, similar to BC and BF. The peak at 1759.06 cm^{-1} could correspond to water stretching vibrations. The peak observed at 563.94 cm^{-1} might be associated with the Fe-OH bending vibrations, indicating the interaction between $FeCl_3$ and the material. It is essential to compare these results to reference spectra of pure bentonite, CaO, and $FeCl_3$ to confirm the presence and interactions of these components in the materials. The FTIR results suggest that these materials contain hydroxyl groups, water molecules, and possible interactions between bentonite and the added compounds (CaO and $FeCl_3$), all of this result showed different characteristic than other materials such as coal and peat as adsorbent (Budihardjo et al., 2021).

Figure 2 also displays the SEM images of each material. In particular, Figures 2(d)-(f) illustrate the morphological characteristics of the materials, highlighting the distinct surface variations among them. In Figure 2(d), a box-like crystalline structure is evident, attributed to the amalgamation of CaO sourced from crab shells. Notably, the heightened CaO concentration correlates with the crystalline presentation and crystal structure (Rezende et al., 2021). Conversely, Figure 2(e) portrays magnetite bentonite, revealing an unaltered surface morphology due to the absence of amalgamation with other solid components. Lastly, Figure 2(f) underscores the synergy between magnetite $FeCl_3$ and CaO from crab shells. Despite the uniform 5000x magnification applied across all figures, discernible disparities in material morphologies persist. This observation unequivocally validates the potential of CaO and $FeCl_3$ to induce modifications in material surface morphologies.

ACCEPTED MANUSCRIPT

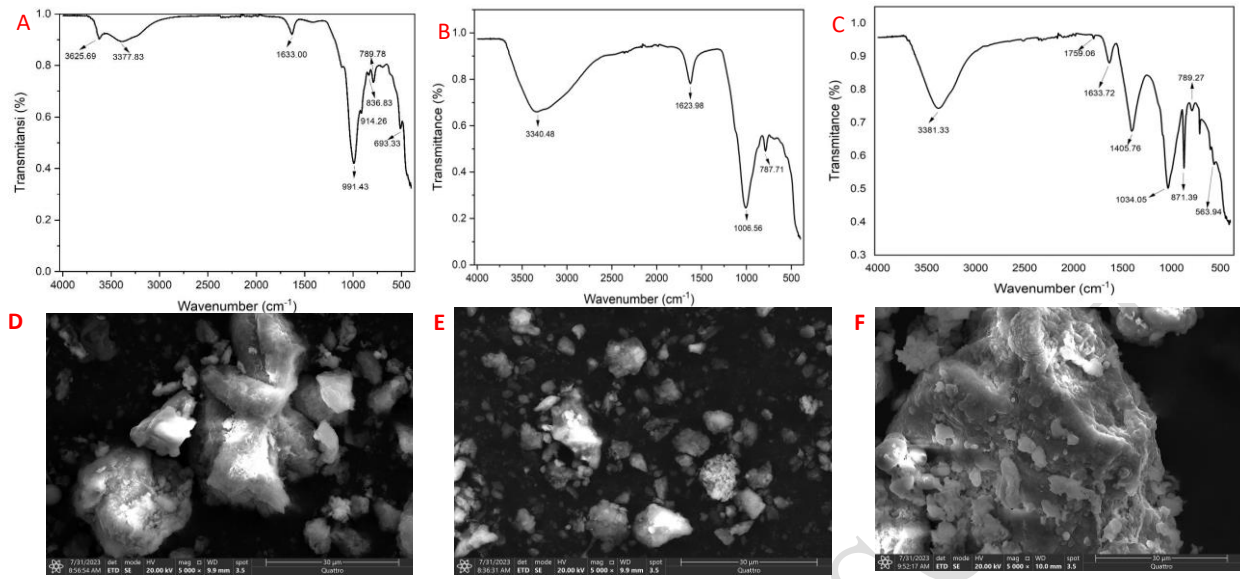

Figure 2. FTIR analyses of BC (a), BF (b), BCF (c) and Photo SEM of BC (d), BF (e) and BCF (f)

Table 1. XRF analyses of materials

Element	Concentration (%)		
	BC	BF	BFC
Si	2.735	2.241	1.476
Ca	12.715	0.382	11.204
Fe	0.388	2.421	1.36
Cl	0.371	14.925	11.067
Al	0.266	0.289	0.154
Ti	0.065	0.075	0.045
Sb	0.031	0.0164	0.024
P	0.248	0.014	0.173
Cd	0.024	0.0117	0.020
Mn	0.033	0.011	0.03
Sn	0.022	0.01	0.018
Zr	0.023	0.006	0.017
Zn	0.003	0.005	0.003
Lightweight elements	82.995	79.013	74.37

ACCEPTED MANUSCRIPT

The N_2 adsorption-desorption isotherm curves presented in **Figure 3** illustrate the textural properties of the synthesized adsorbents, including Bentonite-CaO, Bentonite-$FeCl_3$, and Bentonite-CaO/$FeCl_3$. The graph plots the quantity of nitrogen adsorbed (cm^3/g STP) as a function of the relative pressure (P/P_0), providing insight into the porosity and surface area characteristics of the materials. The adsorption and desorption curves exhibit a characteristic type IV isotherm with an H3 hysteresis loop, indicating the presence of mesoporous structures within the materials (Ribeiro dos Santos et al., 2019). This suggests that the adsorbents possess slit-like pores, which is typical for layered materials such as bentonite. The observed hysteresis loop at higher relative pressures ($P/P_0 > 0.4$) suggests capillary condensation within the mesopores, confirming the presence of interconnected pore structures that facilitate adsorption (Oussalah et al., 2019). Among the three adsorbents, Bentonite-$FeCl_3$ shows the highest adsorption capacity, as evidenced by its greater N_2 uptake at increasing relative pressures. This indicates a more developed pore structure and a higher surface area compared to the other two materials (Cheng et al., 2019). The Bentonite-CaO/$FeCl_3$ composite exhibits a slightly lower adsorption capacity than Bentonite-$FeCl_3$ but still demonstrates significant porosity, suggesting that the combination of CaO and $FeCl_3$ modifications introduces additional functional groups while preserving the material's textural properties (Shattar et al., 2020).

The steep increase in adsorption at high relative pressures ($P/P_0 > 0.9$) across all samples suggests the presence of macropores or large mesopores, which contribute to enhanced diffusion of adsorbate molecules. This characteristic is crucial for practical adsorption applications, as it facilitates rapid uptake of pollutants such as methylene blue (Bakhtiary et al., 2013). The desorption branches of the isotherms do not completely overlap with the adsorption branches, further confirming the presence of mesopores and indicating potential multilayer adsorption or weak physical interactions between nitrogen molecules and the surface (Elkhalifah et al., 2015). Overall, the results confirm that the synthesized bentonite-based adsorbents possess high surface area and mesoporous structures, making them effective for adsorption applications. The presence of $FeCl_3$ appears to enhance porosity and adsorption capacity, while the inclusion of CaO influences the structural and textural properties. These findings align with the observed high efficiency of these

ACCEPTED MANUSCRIPT

materials in methylene blue removal, as a larger surface area and well-developed pore structure enhance adsorption kinetics and overall performance.

The specific surface area of different bentonite composites was analyzed using BET analysis and the results are presented in Table 2. Among the tested composites, Bentonite-$FeCl_3$ exhibited the highest surface area when compared to both Bentonite-CaO and Bentonite-CaO/$FeCl_3$ composites. This superior performance can be attributed to the presence of CaO nanomaterials that effectively filled the pores and increased the surface area of bentonite. Furthermore, the magnetite bentonite-$FeCl_3$ composite demonstrated a unique advantage as its pores and surface area remained unobstructed by other solid materials. This uninhibited configuration likely contributed to the observed higher values of pore diameter and surface area in comparison to the acid-activated bentonite reported in a previous study (Amari et al., 2010)

It is important to note that the increased surface area and pore diameters found in the Bentonite-$FeCl_3$ composite can significantly enhance its sorption abilities. Higher values of these variables generally lead to improved sorption efficiency, making this composite a promising candidate for various sorption applications. However, to comprehensively assess the practical applicability of these bentonite composites, further investigations are warranted. It is essential to study their sorption capacities for specific contaminants and under various environmental conditions. Additionally, understanding the potential impact of other physicochemical properties, such as particle size, morphology, and chemical composition, on the overall sorption performance would provide a more comprehensive understanding of their capabilities.

ACCEPTED MANUSCRIPT

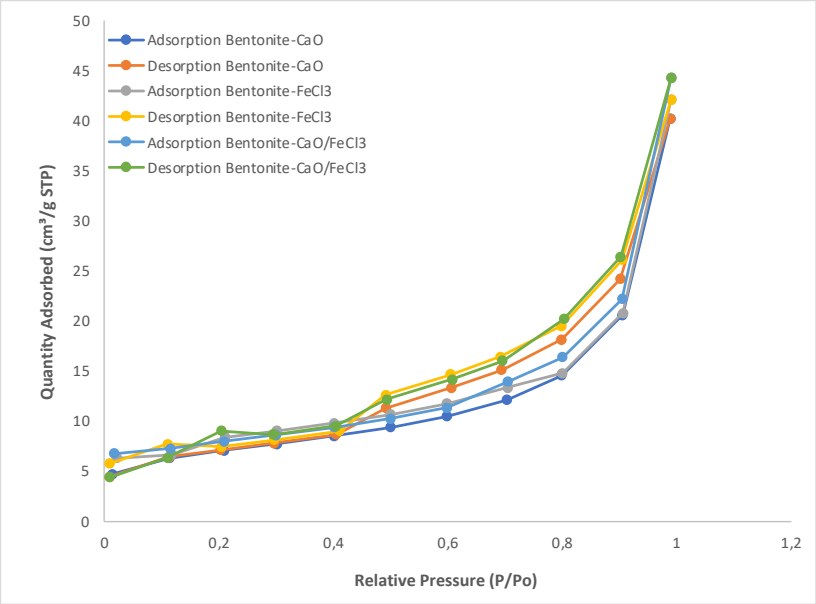

Figure 3. N_2 adsorption-desorption properties

Table 2. Summary report of BET test

Materials	BET Surface Area ($m^2\ g^{-1}$)	Pore volume ($cm^3\ g^{-1}$)	Pore size (nm)
Bentonite-CaO	247.788	0.065	10.512
Bentonie-$FeCl_3$	255.362	0.067	11.110
Bentonite-CaO/$FeCl_3$	238.498	0.062	10.428

ACCEPTED MANUSCRIPT

3.2 Performance Test

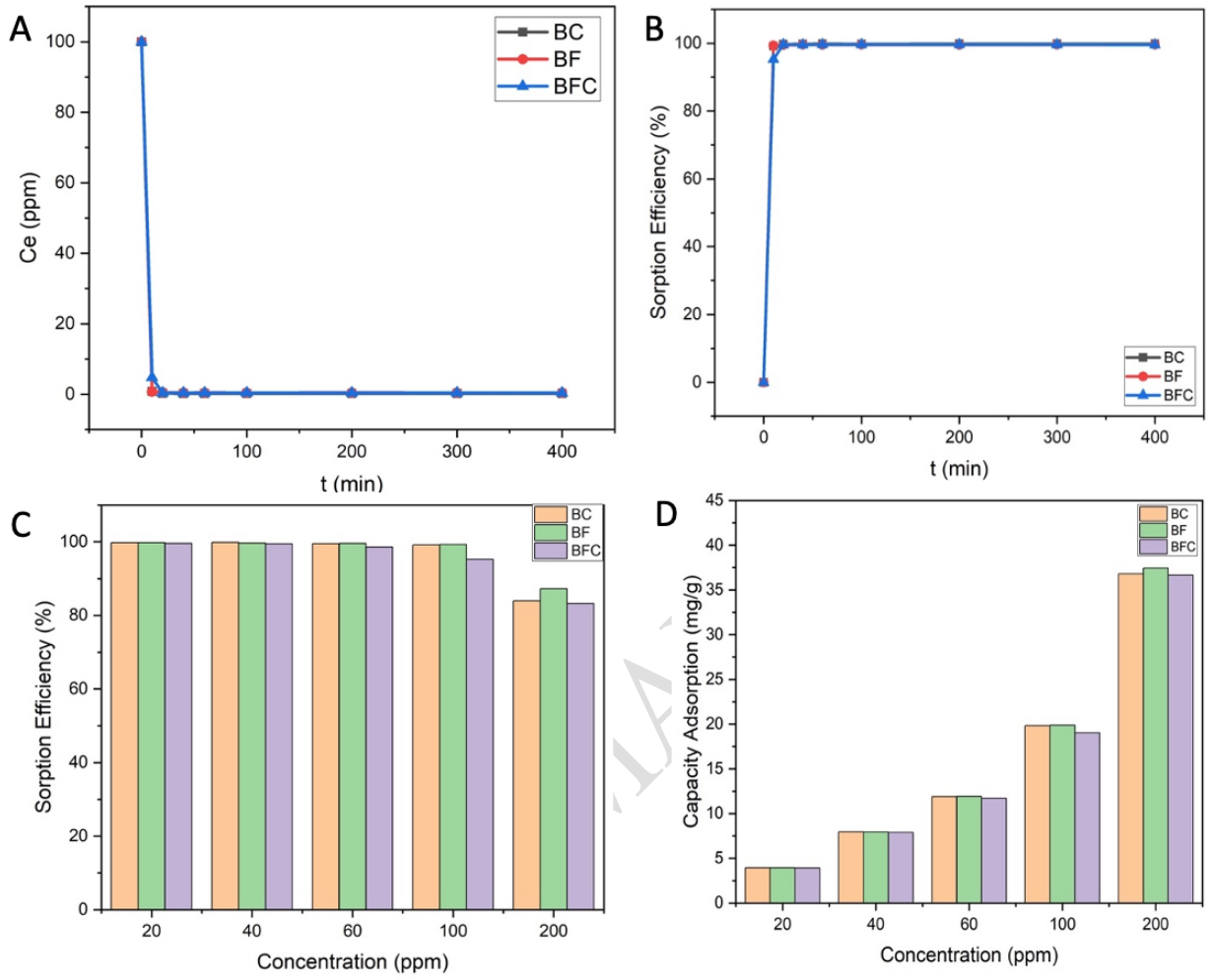

Figure 4. Performance test according to contact times (a), percent removal (b), different concentrations (c), and sorption capacity (d)

Figure 4 presents essential information regarding the materials' performance. In **Figure 4(a)**, the material performance is depicted concerning contact times. Notably, these materials demonstrate impressive capabilities for the efficient removal of methylene blue. Particularly remarkable results are observed after only 10 minutes of contact time, thus affirming their potential as effective agents for anionic dye removal. These findings align with previous studies that utilized modified bentonite for methylene blue removal (Şahin et al., 2015). Additionally, other studies have also corroborated that modified bentonite serves as a highly effective adsorbent for methylene blue (Benhouria et al., 2015)

Figure 4(b) illustrates the sorption efficiency of the materials, which complements the results seen in **Figure 4(a)**, further confirming their remarkable performance. These materials achieve up to 99% removal of methylene blue in just 10 minutes. Furthermore, it is worth noting that Bentonite exhibits outstanding performance even under modification conditions. A recent study demonstrates that an increase in bentonite content added to hydrogel leads to even higher removal rates (Aljar et al., 2021). As the contact time extended, the adsorption rate gradually slowed down, indicating that a portion of the active sites on the bentonite became saturated with adsorbed methylene blue molecules. At this stage, further removal of methylene blue from the solution required more time as the remaining active sites needed to be fully utilized. The results revealed that the removal of methylene blue by these materials increased as the contact time between the solution and adsorbent increased. Initially, the adsorption rate was rapid, with a significant reduction in methylene blue concentration observed within the first few minutes of contact. This suggests that there are abundant active sites on the bentonite surface, enabling rapid binding of methylene blue molecules.

Figure 4(c) showed sorption efficiency of materials according to different concentration of dye. The high sorption efficiency showed the high surface area and pores of materials (Table 2). The surface area of bentonite, often highly charged due to its clay mineral composition, attracts the positively charged methylene blue molecules through electrostatic interactions (Bergaoui et al., 2018). This electrostatic attraction results in the sorption of methylene blue onto the surface of the bentonite particles. Additionally, van der Waals forces and London dispersion forces also play a role in the adsorption process (Sharifi-Bonab et al., 2020). These weak attractive forces contribute to the adherence of methylene blue molecules to the surface and pores of the bentonite. The combination of both physical adsorption (adsorption within the pores) and chemical adsorption (adsorption onto the surface) enhances the overall removal efficiency of methylene blue by bentonite. This multi-layer adsorption mechanism allows bentonite to achieve high adsorption capacity and rapid removal rates, especially during the initial stages of contact time. The strong affinity of bentonite for methylene blue and its ability to accommodate a large number of dye molecules within its porous structure contribute to the impressive performance of methylene blue removal observed in this study.

ACCEPTED MANUSCRIPT

The materials' strong adsorption capabilities, as demonstrated in this study, suggest that they may be well-suited for capturing and removing heavy metal ions from contaminated wastewater. The same principles of adsorption that make them effective for methylene blue removal can be extended to target heavy metal pollutants. Heavy metals are a particularly concerning class of contaminants due to their toxicity and persistence in the environment (Wibowo et al., 2023a). They often find their way into industrial wastewater streams, posing serious health and environmental risks (Sankhla et al., 2016; World Health Organization, 2019). Utilizing the materials studied here for heavy metal adsorption could prove to be a sustainable and efficient solution for mitigating heavy metal pollution in industrial effluents.

Figure 4(d) presents the sorption capacity of the materials at different initial concentrations of methylene blue, revealing a direct correlation between dye concentration and the sorption capacity of the materials, in agreement with findings from a previous study by Kuang et al., 2020. As the initial dye concentration increases, so does the adsorption capacity of the materials. This relationship is expected, as higher dye concentrations provide a greater number of available molecules for adsorption onto the active sites of the adsorbent. The study's results underscore the materials' remarkable ability to efficiently capture methylene blue molecules, irrespective of the dye concentration. This attribute holds significant practical implications, particularly in real-world wastewater treatment applications where pollutant concentrations can vary widely. The observed concentration effect is expected and consistent with typical adsorption behaviour. At low initial concentrations, the adsorbent's active sites may not be fully utilized, leading to lower adsorption capacities. As the concentration increases, more active sites become occupied, resulting in enhanced adsorption capacity. The concentration effect is crucial in real-world applications, as it influences the performance of adsorption systems in treating wastewater with varying pollutant concentrations. In practical scenarios, wastewater streams can exhibit fluctuations in pollutant levels, and the adsorbent's ability to efficiently capture pollutants across a range of concentrations is of paramount importance.

The sorption capacity of the materials investigated in this study demonstrates notable performance, with BF exhibiting the highest maximum sorption capacity at 38 mg g^{-1}. This capacity surpasses that of other materials, such as wood millet carbon (2.9 mg g^{-1}) (Ghaedi and Kokhdan, 2015), and sugar extracted spent rice biomass (8.13 mg g^{-1}) (Rehman et al., 2012). The superiority of BF's

ACCEPTED MANUSCRIPT

sorption capacity can be attributed to the magnetic modification incorporated into this material, which enhances its affinity for methylene blue molecules. The magnetic modification in BF facilitates the attraction and binding of a greater number of methylene blue molecules compared to the other materials. This suggests that BF offers more accessible active sites and a higher surface area for methylene blue adsorption. On the other hand, BFC, despite also containing magnetite, incorporates the additional component of CaO, which may fill and obstruct the pores and surface area of the adsorbent. Consequently, the sorption capacity of BFC is comparatively lower than that of BF.

The magnetic modification in BF holds promise for various applications, as it enables effective capture of methylene blue and potentially other pollutants. The magnetic properties allow for easy separation of the adsorbent from the treated wastewater using a magnetic field, facilitating the recovery and reuse of the adsorbent material. It is worth noting that the sorption capacities reported in this study provide valuable insights into the materials' performance in methylene blue removal. However, further investigation is necessary to understand the materials' long-term stability, reusability, and regeneration potential. Exploring these aspects would contribute to optimizing the practical implementation of these materials in sustainable and cost-effective wastewater treatment processes.

3.3 Adsorption Isotherm

In order to assess the adsorption characteristics of the materials, this research utilized five distinct isotherm models: Langmuir, Freundlich, BET, Temkin, and Dubinin-Radushkevich. The Langmuir isotherm exhibited a remarkable correspondence with each of the materials, as indicated by the correlation coefficient (*R2*) value of 0.9999 (**Figure 5**). The Langmuir isotherm model offers significant contributions to the understanding of the capacity of monolayer adsorption and the interplay between the adsorbent (materials) and the adsorbate (methylene blue). Without any interaction between adsorbed molecules, it posits a finite number of identical adsorption sites and a homogeneous surface. The experimental data exhibit a close correspondence with the theoretical predictions of the Langmuir model, as evidenced by the high *R2* value.

The congruence of the results obtained in this study, where bentonite materials effectively adsorb methylene blue following the Langmuir model, with a previous study that used the same material for the adsorption of Cu^{2+} and Ni^{2+} (Liu and Zhou, 2010), is highly noteworthy. The fact that both

ACCEPTED MANUSCRIPT

studies fitted well with the Langmuir model suggests that the adsorption behaviour of bentonite is consistent and predictable across different adsorbates, namely Cu^{2+}, Ni^{2+} and methylene blue. The successful implementation of the Langmuir model in both investigations suggests that the process by which these metal ions and methylene blue are adsorbed onto bentonite can be characterized as monolayer adsorption occurring on a uniform surface containing a finite number of identical adsorption sites. This indicates that the adsorbate molecules adhere to the bentonite surface in a single layer, and that no interaction occurs between the adsorbed species.

The similarity in the adsorption mechanism for both metal ions and methylene blue highlights the versatility and effectiveness of bentonite as an adsorbent for various pollutants, regardless of their chemical nature. This is particularly valuable in the context of wastewater treatment, where the presence of multiple pollutants is common. The ability of bentonite to effectively remove both metal ions and organic dyes, such as methylene blue, suggests that it can be employed as a multifunctional adsorbent in diverse wastewater treatment scenarios. Furthermore, the consistent application of the Langmuir model in both studies allows for easy comparison of adsorption capacities and affinities across different adsorbates.

According to the Langmuir isotherm model, at a specific temperature, the adsorption process reaches a point where the adsorbent's active sites become fully occupied by the adsorbate, leading to monolayer coverage. This implies that further increases in methylene blue concentration will not result in additional adsorption as all available sites are already utilized. The monolayer adsorption capacity (*Qmax*) obtained from the Langmuir isotherm provides valuable information about the maximum amount of methylene blue that can be adsorbed per unit weight of the adsorbent. This parameter is crucial for determining the efficiency and potential application of the materials for wastewater treatment. By employing the Langmuir isotherm model, this study offers valuable insights into the adsorption mechanism and the materials' ability to form a monolayer of methylene blue on their surface. The high R^2 value indicates the accuracy and reliability of the model in describing the adsorption behaviour of the materials.

By employing various isotherm models—Langmuir, Freundlich, BET, Temkin, and Dubinin-Radushkevich—this research offers an exhaustive comprehension of the materials' methylene blue adsorption characteristics. Every isotherm model provides distinct perspectives on the adsorption mechanism and aids in the characterization of the methylene blue-adsorbent interaction.

ACCEPTED MANUSCRIPT

Assuming a finite number of identical adsorption sites on a homogeneous surface, the Langmuir isotherm predicts monolayer adsorption. It implies that equilibrium is reached in the adsorption process when the adsorbate completely occupies all active sites on the adsorbent surface. The underlying premise of the model is the absence of any interaction among the molecules that are adsorbed. The monolayer adsorption capacity (*Qmax*) and the Langmuir constant (K_L), which signifies the adsorbate's affinity for the adsorbent, are both expressed in the Langmuir isotherm equation. Conversely, the Freundlich isotherm delineates heterogeneous adsorption occurring at a surface characterized by varying adsorption energies through the use of an empirical model. Comparable to the Langmuir model, it accommodates adsorption on heterogeneous surfaces and is more flexible. The adsorption capacity (K_F) and the intensity of adsorption (*n*), which define the adsorption strength and surface heterogeneity, are parameters of the Freundlich isotherm equation.

Particularly pertinent to physical adsorption on porous surfaces is the BET isotherm. It operates under the assumption of multilayer adsorption, wherein the interaction between the adsorbed molecules and the adsorbate generates each layer. The model is frequently applied to specific surface area of porous material calculations. The monolayer capacity (*Qm*) and the BET constant (*C*) are crucial parameters in determining the adsorption capacity and porosity of materials, respectively. The Temkin isotherm, which assumes a linear reduction in the heat of adsorption as coverage increases, considers the interactions that occur between the adsorbate and the adsorbent. This analysis takes into account the consequences of interactions between the adsorbent and the adsorbate and offers valuable insights into the characteristics of adsorption mechanisms. The Temkin constant (*B*) and the heat of adsorption (*A*) are derived from the Temkin isotherm equation, which offers significant insights into the kinetics of the adsorption process.

The Dubinin-Radushkevich isotherm is primarily used to analyze adsorption onto heterogeneous surfaces through the application of the Dubinin-Radushkevich equation. It characterizes the adsorption process in terms of the sorption energy and the Polanyi potential, which are useful for understanding the mechanism of adsorption onto heterogeneous surfaces. By employing these various isotherm models, this study gains a comprehensive understanding of the adsorption behaviour of the materials and their potential for methylene blue removal. Each model provides unique information about adsorption capacity, surface heterogeneity, adsorption energetics, and porosity, enhancing the overall understanding of the materials' adsorption capabilities. The

ACCEPTED MANUSCRIPT

combined use of these isotherm models helps researchers to better tailor and optimize adsorbents for practical applications in wastewater treatment and environmental remediation processes.

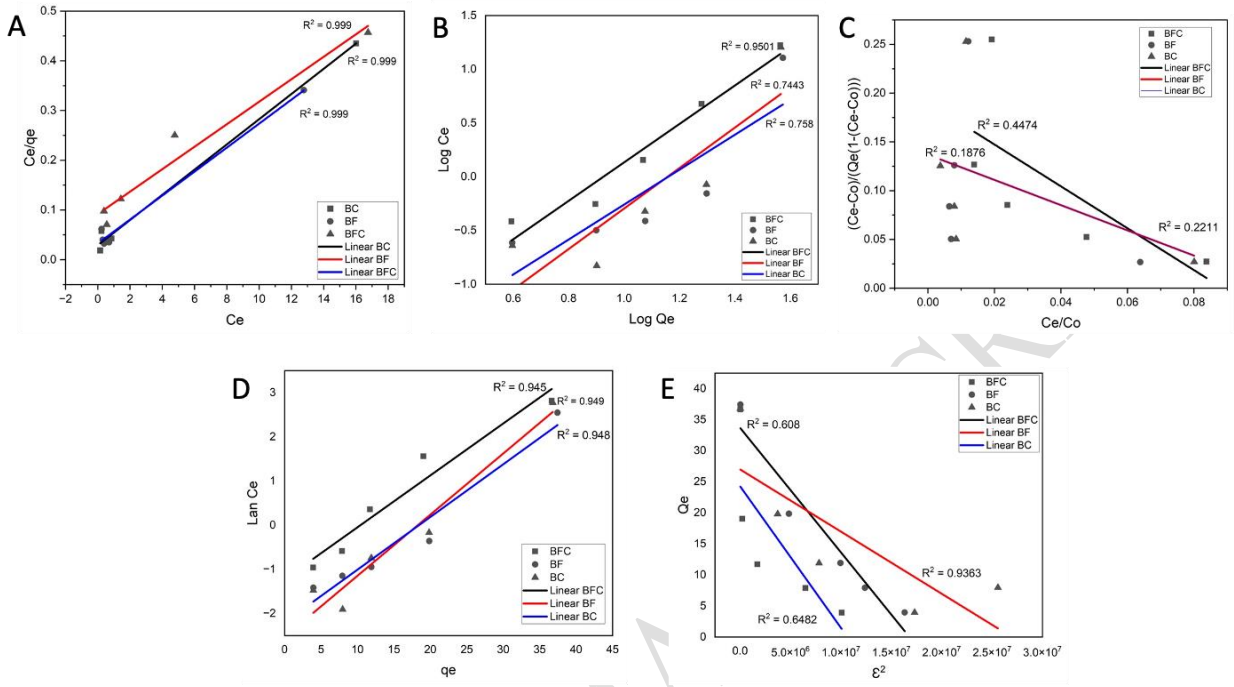

Figure 5. Isotherm model of (a) Langmuir, (b) Freundlich, (c) BET, (d) Temkin and (e) Dubinin-Radushkevich

3.4 Kinetics

The results of the kinetic experiments performed on the materials are illustrated in **Figure 6**. A thorough investigation of kinetics was conducted in this study, which included the utilization of second-order, pseudo-first-order, and pseudo-zero-order kinetic models. The results of this examination are of the utmost importance, as they reveal vital details regarding the properties of the sorption process involving the substances and methylene blue. By utilizing the pseudo-zero-order, pseudo-first-order, and second-order kinetic models, the kinetic experiments analyze the dynamic behaviour of the adsorption process for particular purposes. The pseudo-zero-order model investigates whether the rate of adsorption is unaffected by the initial concentration of methylene blue; this provides insight into potential rate-limiting phases and process-influencing factors. Understanding the initial adsorption rate and the interaction between the adsorbate and adsorbent in the early phases of adsorption is facilitated by the pseudo-first order model. In contrast, the second-order kinetic model offers valuable insights regarding the comprehensive adsorption rate,

as well as the critical values of adsorbate concentration and adsorption site accessibility on the adsorbent surface.

According to the test results, all materials in this study exhibited an excellent fit with the pseudo second-order kinetic model. This finding indicates that the rate of adsorption is dependent on both the concentration of methylene blue and the availability of adsorption sites on the materials' surfaces. The successful fit with the pseudo second-order model implies that the adsorption process follows a second-order reaction, indicating that the interaction between the materials and methylene blue is robust and efficiently takes place on the materials' surfaces. The consistency of the pseudo second order fit across all materials underscores their effectiveness as adsorbents for methylene blue removal. This suggests that the materials have ample active sites and are capable of efficiently capturing methylene blue molecules.

Result of this study showed the relevant with previous study using plasma surface modified bentonite for removal of methylene blue (Şahin et al., 2015) In other side, previous study also showed the pseudo second order for acid dyes removal using acid-activated bentonite (Özcan and Özcan, 2004). This fact not only followed the bentonite materials, several previous studies also showed the same result for carbon base materials such as green biochar/iron oxide composite for methylene blue removal (Zhang et al., 2020), magnetite-activated-biochar nanocomposite also in methylene blue application (Yao et al., 2020) and anaerobic granular sludge-based biochar (Shi et al., 2014) and clay materials such as natural zeolite (Han et al., 2009), zeolite synthesized from fly ash (Fungaro et al., 2009), nanocrystal zeolite (Sohrabnezhad and Pourahmad, 2010), kaolin (Rida et al., 2013) and kaolin with graphene oxide modification (He et al., 2018b).

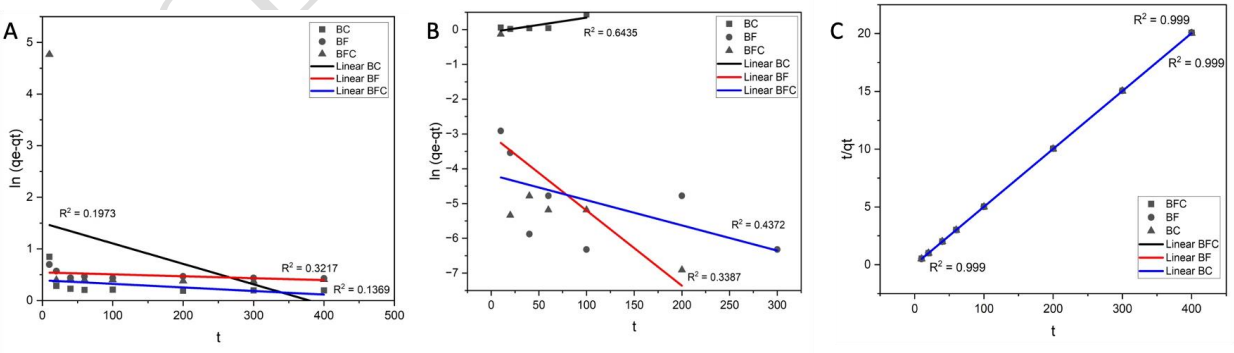

Figure 6. pseudo zero-order (a), pseudo first-order (b) and pseudo second order (c)

3.6 Thermodynamic Analysis

Thermodynamic analysis plays a crucial role in understanding and characterizing the adsorption process (Anastopoulos and Kyzas, 2016). Thermodynamic analysis provides valuable insights into the energetics and feasibility of the adsorption process (Saha et al., 2010). For BC, the $\Delta G = 1.200$ kJ mol^{-1}, which indicates that the reaction is not spontaneous under standard conditions ($\Delta G > 0$). However, the value is relatively small, so the reaction might still occur at non-standard conditions if ΔG becomes negative (e.g., by changing temperature or pressure). $\Delta H = 93.6175387$ kJ mol^{-1}, which shows that the reaction is endothermic since the enthalpy change is positive. This means that heat is absorbed from the surroundings during the reaction. $\Delta S = 306.080991$ J K^{-1} mol^{-1}, indicating an increase in disorder or randomness in the system during the reaction. Secondly, for BF $\Delta G = 1.326$ kJ mol^{-1}, again suggesting that the reaction is not spontaneous under standard conditions. $\Delta H = 116.488706$ kJ mol^{-1}, indicating that this reaction is also endothermic, absorbing heat from the surroundings. $\Delta S = 377.440385$ J K^{-1} mol^{-1}, which is a higher increase in entropy compared to the first reaction, suggesting a greater increase in disorder. The last for BCF is $\Delta G = -2.004$ kJ mol^{-1}, indicating that the reaction is spontaneous under standard conditions. A negative ΔG means that the reaction can proceed spontaneously without the need for additional energy input. $\Delta H = 32.237876$ kJ mol^{-1}, indicating that this reaction is exothermic, releasing heat to the surroundings. $\Delta S = 111.885821$ J K^{-1} mol^{-1}, representing an increase in entropy but to a lesser extent than in BF.

Thus, the provided data gives us insights into the spontaneity and energy changes involved in these reactions. BCF stands out as being spontaneous and exothermic, with a moderate increase in entropy. BC and BF, on the other hand, are not spontaneous under standard conditions, with BF having a higher increase in entropy compared to reaction BC. However, non-spontaneous reactions can still occur under non-standard conditions if the appropriate factors (temperature, pressure, concentration) are adjusted to make ΔG negative. Thermodynamic analysis is a powerful tool for gaining a deeper understanding of the adsorption process. It provides fundamental information about the driving forces, stability, and energy changes involved in adsorption, enabling researchers to design more efficient adsorption systems for various applications, such as water purification, gas separation, and environmental remediation like this study.

Table 3. Thermodynamic parameters

ACCEPTED MANUSCRIPT

Material	Intercept	Slope	R^2	R ($J.mol^{-1}.K^{-1}$)	ΔG ($KJ.mol^{-1}$)	ΔH ($KJ.mol^{-1}$)	ΔS ($J.K^{-1}.mol^{-1}$)
BC	36.815	-11260.228	0.9127	8.314	1.200	93.617	306.08
BF	45.398	-14011.150	0.8615	8.314	1.326	116.488	377.44
BCF	13.457	-3877.5410	0.9961	8.314	-2.004	32.237	111.885

3.7 Mechanism of Pollutants Removal

The adsorption mechanism of MB onto the modified bentonite composites—BC, BF, and BFC—is governed by multiple interactions, including electrostatic attraction, ion exchange, surface complexation, and physical adsorption (**Figure 7**). The synergistic effect of the modifications with CaO and $FeCl_3$ enhances the removal efficiency by altering the physicochemical properties of the adsorbents. Electrostatic interactions play a dominant role in the adsorption process due to the negatively charged surface of bentonite, which attracts the positively charged MB molecules in aqueous solution. The isomorphous substitution of Si^{4+} by Al^{3+} in the tetrahedral layer and Al^{3+} by Mg^{2+} in the octahedral layer creates permanent negative charges on the bentonite surface, further intensified by the presence of $FeCl_3$, which increases charge density and enhances adsorption (Gupta et al., 2015b).

ACCEPTED MANUSCRIPT

Figure 7. Removal mechanism of MB into the materials

Another crucial mechanism is ion exchange, where exchangeable cations such as Na^{+}, Ca^{2+}, and Mg^{2+} in the natural bentonite structure are replaced by MB^{+} cations. The BC introduces additional alkaline sites, facilitating cation exchange by promoting the replacement of Ca^{2+} ions with MB^{+} molecules. This process contributes to the overall adsorption capacity and enhances the efficiency of MB removal (De Castro et al., 2018b). In addition to electrostatic attraction and ion exchange, surface complexation significantly influences MB adsorption. The introduction of $FeCl_3$ leads to the formation of iron oxides and hydroxides on the bentonite surface, which serve as additional adsorption sites. FTIR analysis confirmed the presence

of hydroxyl (-OH) and Fe-OH functional groups, which promote hydrogen bonding and ligand exchange interactions with MB molecules. The Fe-O bonds facilitate the removal of MB through ligand exchange, where hydroxyl groups on Fe sites are replaced by MB molecules, further increasing adsorption efficiency (Lou et al., 2015).

Physical adsorption also plays an important role in the process, with van der Waals forces and pore-filling mechanisms contributing to MB capture. BET analysis revealed that the modified bentonite composites exhibited increased surface area and pore volume, allowing for the diffusion of MB molecules into the porous structure (Ranđelović et al., 2014). The presence of CaO, derived from crab shells, contributes to increased surface roughness and pore heterogeneity, enabling enhanced multilayer adsorption. The combination of CaO and $FeCl_3$ modification in BFC results in superior adsorption performance due to the complementary mechanisms of ion exchange, electrostatic attraction, and surface complexation. The presence of $FeCl_3$ enhances charge-assisted interactions, while CaO modification provides additional binding sites for MB removal. Thermodynamic analysis further confirmed that adsorption onto BFC follows a spontaneous and exothermic process, highlighting the strong affinity between MB molecules and the modified adsorbents (Hong et al., 2009).

Compared to unmodified bentonite, the improved adsorption capacity of the modified bentonite composites is attributed to higher negative surface charge density due to $FeCl_3$ modification, increased availability of alkaline sites from CaO, enhanced surface functional groups (Fe-OH and Ca-OH) promoting chemisorption, and larger surface area and pore volume enabling efficient MB diffusion. These combined mechanisms ensure that the modified magnetite bentonite-CaO/$FeCl_3$ composite acts as a highly efficient and cost-effective adsorbent for MB removal, providing a sustainable solution for wastewater treatment applications.

3.8 Future Prospect and Recommendation

This study has provided valuable insights into the adsorption capabilities of the investigated materials (BC, BF, and BFC) for methylene blue removal. The successful application of the Langmuir isotherm and the pseudo-second-order kinetic model indicates that these materials possess high adsorption capacities and rapid adsorption kinetics, making them promising candidates for wastewater treatment applications. Further mechanistic studies should be conducted to deepen the understanding of the adsorption mechanisms. Investigating the surface chemistry, morphology, and pore structure of the materials could elucidate specific interactions between the adsorbents and methylene blue, providing valuable insights into the governing adsorption

ACCEPTED MANUSCRIPT

mechanisms. Fine-tuning the adsorption conditions, such as pH, temperature, and contact time, can enhance the efficiency and effectiveness of the materials in methylene blue removal. Conducting systematic optimization studies will help determine the optimal conditions for practical applications.

Assessing the regeneration potential and reusability of the adsorbents is crucial for sustainable wastewater treatment processes. Investigating methods to regenerate the materials and retain their adsorption capacity over multiple cycles could improve their economic viability and reduce environmental impacts. In addition, validating the materials' performance using real wastewater samples is essential to demonstrate their practical applicability. Assessing the performance of these materials with real wastewater containing various pollutants, as well as comparing it's performance with other commercially available adsorbents, will provide valuable. If the materials exhibit excellent performance and cost-effectiveness in laboratory-scale experiments, further scale-up studies should be conducted to assess their feasibility for large-scale wastewater treatment applications.

In other side, some recommendation needs to be developed including considering the exceptional adsorption capacities and rapid kinetics of the materials, they should be explored for practical applications in wastewater treatment, especially for the removal of methylene blue and other organic dyes. Collaborations with relevant industries and wastewater treatment facilities can facilitate the implementation of these materials in real-world scenarios. Although the materials have demonstrated promising results in laboratory settings, it is essential to assess their potential environmental impact when used in large-scale applications. Environmental and health risk assessments should be conducted to ensure the safe use of these materials. To unlock the full potential of these materials, further research should be undertaken to investigate their performance against other pollutants, such as heavy metals and organic compounds. Understanding their broader adsorption capabilities will expand their application possibilities and the last recommendation is performing a comprehensive cost-benefit analysis will help evaluate the economic feasibility of using these materials in wastewater treatment processes. Comparing the costs of production, implementation, and regeneration with the benefits of efficient pollutant removal will aid in making informed decisions.

ACCEPTED MANUSCRIPT

4. Conclusion

This study successfully investigated the adsorption capabilities of novel modified bentonite adsorbents—Bentonite-CaO (BC), Bentonite-$FeCl_3$ (BF), and Bentonite-CaO/$FeCl_3$ (BFC)—for the removal of methylene blue (MB) from aqueous solutions. The materials were synthesized using bentonite and crab shell waste, with modifications involving $FeCl_3$ and CaO, enhancing their adsorption efficiency. Characterization using FTIR confirmed the presence of hydroxyl (-OH) and Fe-OH functional groups, which played a crucial role in adsorption through hydrogen bonding and ligand exchange interactions. XRF analysis showed that the modification process introduced significant elemental variations, with Fe concentrations increasing from 0.388% in BC to 2.421% in BF and 1.36% in BFC, while Ca concentrations varied, contributing to changes in adsorption performance. BET surface area analysis revealed that BF exhibited the highest surface area of 255.36 m^2/g, followed by BC at 247.79 m^2/g and BFC at 238.50 m^2/g, demonstrating the impact of modification on pore structure and adsorption efficiency. The adsorption performance tests demonstrated exceptional efficiency, achieving a 99% removal of methylene blue within just 10 minutes. The maximum adsorption capacity was recorded at 39 mg/g, significantly higher than many conventional adsorbents. Kinetic studies confirmed that the adsorption process followed a pseudo-second-order kinetic model, indicating that the adsorption rate was dependent on both the MB concentration and the availability of adsorption sites. Isotherm modeling showed that the Langmuir isotherm model provided the best fit ($R^2 = 0.9999$), confirming monolayer adsorption on a homogeneous surface, with a maximum adsorption capacity higher than many previously reported bentonite-based adsorbents.

Thermodynamic analysis revealed that the adsorption process exhibited different behaviors depending on the material used. While BFC demonstrated spontaneous and exothermic adsorption ($\Delta G = -2.004$ kJ/mol, $\Delta H = 32.24$ kJ/mol, $\Delta S = 111.89$ J/K/mol), both BC and BF were non-spontaneous under standard conditions but had a strong entropic driving force, suggesting that adsorption could be facilitated under optimized environmental conditions. The study highlighted that BFC, due to its synergistic combination of $FeCl_3$ and CaO modifications, exhibited the highest adsorption efficiency, making it the most promising candidate for large-scale wastewater treatment applications. Future studies should focus on optimizing adsorption conditions such as pH, temperature, and contact time to maximize removal efficiency. Additionally, investigating the reusability and regeneration potential of these adsorbents will be critical for sustainable application. The results indicate that these novel modified bentonite composites have strong potential for real-world wastewater treatment, providing a low-cost, eco-friendly, and highly effective solution for dye removal. Further research should also explore the application of these materials for the removal of other organic and inorganic pollutants, expanding their applicability in environmental remediation.

5. Statement and Declaration

The authors confirmed there is no conflict of interest in this study.

6. Data Availability

All data published in this article will be made available upon request.

ACCEPTED MANUSCRIPT

7. Reference

Aljar, M.A.A., Rashdan, S., El-Fattah, A.A., 2021. Environmentally friendly polyvinyl alcohol−alginate/ bentonite semi-interpenetrating polymer network nanocomposite hydrogel beads as an efficient adsorbent for the removal of methylene blue from aqueous solution. Polymers (Basel) 13. https://doi.org/10.3390/polym13224000

Alsukaibi, A.K.D., 2022. Various Approaches for the Detoxification of Toxic Dyes in Wastewater. Processes. https://doi.org/10.3390/pr10101968

Al-Tohamy, R., Ali, S.S., Li, F., Okasha, K.M., Mahmoud, Y.A.G., Elsamahy, T., Jiao, H., Fu, Y., Sun, J., 2022. A critical review on the treatment of dye-containing wastewater: Ecotoxicological and health concerns of textile dyes and possible remediation approaches for environmental safety. Ecotoxicol Environ Saf. https://doi.org/10.1016/j.ecoenv.2021.113160

Amari, A., Chlendi, M., Gannouni, A., Bellagi, A., 2010. Optimised activation of bentonite for toluene adsorption. Appl Clay Sci 47, 457–461. https://doi.org/10.1016/j.clay.2009.11.035

Anastopoulos, I., Kyzas, G.Z., 2016. Are the thermodynamic parameters correctly estimated in liquid-phase adsorption phenomena? J Mol Liq 218, 174–185. https://doi.org/10.1016/j.molliq.2016.02.059

Asuha, S., Fei, F., Wurendaodi, W., Zhao, S., Wu, H., Zhuang, X., 2020. Activation of kaolinite by a low-temperature chemical method and its effect on methylene blue adsorption. Powder Technol 361, 624–632. https://doi.org/10.1016/j.powtec.2019.11.068

Awad, H.E.A., Mohammad, A.M., Farahat, E.A., 2023. Potential use of dry powder of Vossia cuspidata (Roxb.) Griff. rhizomes and leaves in methylene blue dye remediation. Sci Rep 13. https://doi.org/10.1038/s41598-023-37987-0

Bakhtiary, S., Shirvani, M., Shariatmadari, H., 2013. Adsorption–desorption behavior of 2,4-D on NCP-modified bentonite and zeolite: Implications for slow-release herbicide formulations. Chemosphere 90, 699–705. https://doi.org/10.1016/j.chemosphere.2012.09.052

Benhouria, A., Islam, M.A., Zaghouane-Boudiaf, H., Boutahala, M., Hameed, B.H., 2015. Calcium alginate-bentonite-activated carbon composite beads as highly effective adsorbent for methylene blue. Chemical Engineering Journal 270, 621–630. https://doi.org/10.1016/j.cej.2015.02.030

Bergaoui, M., Nakhli, A., Benguerba, Y., Khalfaoui, M., Erto, A., Soetaredjo, F.E., Ismadji, S., Ernst, B., 2018. Novel insights into the adsorption mechanism of methylene blue onto organo-bentonite: Adsorption isotherms modeling and molecular simulation. J Mol Liq 272, 697–707. https://doi.org/10.1016/j.molliq.2018.10.001

Bestani, B., Benderdouche, N., Benstaali, B., Belhakem, M., Addou, A., 2008. Methylene blue and iodine adsorption onto an activated desert plant. Bioresour Technol 99, 8441–8444. https://doi.org/10.1016/j.biortech.2008.02.053

Boretti, A., Rosa, L., 2019. Reassessing the projections of the World Water Development Report. NPJ Clean Water 2. https://doi.org/10.1038/s41545-019-0039-9

Budihardjo, M.A., Wibowo, Y.G., Ramadan, B.S., Serunting, M.A., Yohana, E., Syafrudin, 2021. Mercury removal using modified activated carbon of peat soil and coal in simulated landfill leachate. Environ Technol Innov 24. https://doi.org/10.1016/j.eti.2021.102022

ACCEPTED MANUSCRIPT

Cheng, H., Zhu, Q., Xing, Z., 2019. Adsorption of ammonia nitrogen in low temperature domestic wastewater by modification bentonite. J Clean Prod 233, 720–730. https://doi.org/10.1016/j.jclepro.2019.06.079

De Castro, M.L.F.A., Abad, M.L.B., Sumalinog, D.A.G., Abarca, R.R.M., Paoprasert, P., de Luna, M.D.G., 2018a. Adsorption of Methylene Blue dye and Cu(II) ions on EDTA-modified bentonite: Isotherm, kinetic and thermodynamic studies. Sustainable Environment Research 28, 197–205. https://doi.org/10.1016/j.serj.2018.04.001

De Castro, M.L.F.A., Abad, M.L.B., Sumalinog, D.A.G., Abarca, R.R.M., Paoprasert, P., de Luna, M.D.G., 2018b. Adsorption of Methylene Blue dye and Cu(II) ions on EDTA-modified bentonite: Isotherm, kinetic and thermodynamic studies. Sustainable Environment Research 28, 197–205. https://doi.org/10.1016/j.serj.2018.04.001

Doke, S.M., Yadav, G.D., 2014. Novelties of combustion synthesized titania ultrafiltration membrane in efficient removal of methylene blue dye from aqueous effluent. Chemosphere 117, 760–765. https://doi.org/10.1016/j.chemosphere.2014.10.029

El-Halwany, M.M., 2010. Study of adsorption isotherms and kinetic models for Methylene Blue adsorption on activated carbon developed from Egyptian rice hull (Part II). Desalination 250, 208–213. https://doi.org/10.1016/j.desal.2008.07.030

Elkhalifah, A.E.I., Azmi Bustam, M., Shariff, A.M., Murugesan, T., 2015. Selective adsorption of CO2 on a regenerable amine-bentonite hybrid adsorbent. Appl Clay Sci 107, 213–219. https://doi.org/10.1016/j.clay.2015.01.030

Farhan Hanafi, M., Sapawe, N., 2019. ScienceDirect The Potential of ZrO 2 Catalyst Toward Degradation of Dyes and Phenolic Compound.

Food and Agriculture Organization of the United Nations, 2020. The State of Food and Agriculture 2020, The State of Food and Agriculture 2020. FAO. https://doi.org/10.4060/cb1447en

Fungaro, D.A., Bruno, M., Grosche, L.C., 2009. Adsorption and kinetic studies of methylene blue on zeolite synthesized from fly ash. Desalination Water Treat 2, 231–239. https://doi.org/10.5004/dwt.2009.305

Ghaedi, M., Kokhdan, S.N., 2015. Removal of methylene blue from aqueous solution by wood millet carbon optimization using response surface methodology. Spectrochim Acta A Mol Biomol Spectrosc 136, 141–148. https://doi.org/10.1016/j.saa.2014.07.048

Gupta, V.K., Sharma, M., Vyas, R.K., 2015a. Hydrothermal modification and characterization of bentonite for reactive adsorption of methylene blue: An ESI-MS study. J Environ Chem Eng 3, 2172–2179. https://doi.org/10.1016/j.jece.2015.07.022

Gupta, V.K., Sharma, M., Vyas, R.K., 2015b. Hydrothermal modification and characterization of bentonite for reactive adsorption of methylene blue: An ESI-MS study. J Environ Chem Eng 3, 2172–2179. https://doi.org/10.1016/j.jece.2015.07.022

Han, R., Zhang, J., Han, P., Wang, Y., Zhao, Z., Tang, M., 2009. Study of equilibrium, kinetic and thermodynamic parameters about methylene blue adsorption onto natural zeolite. Chemical Engineering Journal 145, 496–504. https://doi.org/10.1016/j.cej.2008.05.003

ACCEPTED MANUSCRIPT

He, K., Chen, G., Zeng, G., Chen, A., Huang, Z., Shi, J., Peng, M., Huang, T., Hu, L., 2018a. Enhanced removal performance for methylene blue by kaolin with graphene oxide modification. J Taiwan Inst Chem Eng 89, 77–85. https://doi.org/10.1016/j.jtice.2018.04.013

He, K., Chen, G., Zeng, G., Chen, A., Huang, Z., Shi, J., Peng, M., Huang, T., Hu, L., 2018b. Enhanced removal performance for methylene blue by kaolin with graphene oxide modification. J Taiwan Inst Chem Eng 89, 77–85. https://doi.org/10.1016/j.jtice.2018.04.013

Hong, S., Wen, C., He, J., Gan, F., Ho, Y.-S., 2009. Adsorption thermodynamics of Methylene Blue onto bentonite. J Hazard Mater 167, 630–633. https://doi.org/10.1016/j.jhazmat.2009.01.014

Islam, M.R., Mostafa, M.G., 2022. Adsorption kinetics, isotherms and thermodynamic studies of methyl blue in textile dye effluent on natural clay adsorbent. Sustain Water Resour Manag 8, 52. https://doi.org/10.1007/s40899-022-00640-1

Kishor, R., Purchase, D., Saratale, G.D., Saratale, R.G., Ferreira, L.F.R., Bilal, M., Chandra, R., Bharagava, R.N., 2021. Ecotoxicological and health concerns of persistent coloring pollutants of textile industry wastewater and treatment approaches for environmental safety. J Environ Chem Eng 9. https://doi.org/10.1016/j.jece.2020.105012

Kuang, Y., Zhang, X., Zhou, S., 2020. Adsorption of methylene blue in water onto activated carbon by surfactant modification. Water (Switzerland) 12. https://doi.org/10.3390/w12020587

Lau, Y.Y., Wong, Y.S., Teng, T.T., Morad, N., Rafatullah, M., Ong, S.A., 2015. Degradation of cationic and anionic dyes in coagulation-flocculation process using bi-functionalized silica hybrid with aluminum-ferric as auxiliary agent. RSC Adv 5, 34206–34215. https://doi.org/10.1039/c5ra01346a

Liu, Z. rong, Zhou, S. qi, 2010. Adsorption of copper and nickel on Na-bentonite. Process Safety and Environmental Protection 88, 62–66. https://doi.org/10.1016/j.psep.2009.09.001

Lou, Z., Zhou, Z., Zhang, W., Zhang, X., Hu, X., Liu, P., Zhang, H., 2015. Magnetized bentonite by Fe3O4 nanoparticles treated as adsorbent for methylene blue removal from aqueous solution: Synthesis, characterization, mechanism, kinetics and regeneration. J Taiwan Inst Chem Eng 49, 199–205. https://doi.org/10.1016/j.jtice.2014.11.007

Mittal, A., Mittal, J., Malviya, A., Gupta, V.K., 2009. Adsorptive removal of hazardous anionic dye "Congo red" from wastewater using waste materials and recovery by desorption. J Colloid Interface Sci 340, 16–26. https://doi.org/10.1016/j.jcis.2009.08.019

Mojoudi, N., Mirghaffari, N., Soleimani, M., Shariatmadari, H., Belver, C., Bedia, J., 2019. Phenol adsorption on high microporous activated carbons prepared from oily sludge: equilibrium, kinetic and thermodynamic studies. Sci Rep 9. https://doi.org/10.1038/s41598-019-55794-4

Oladoye, P.O., Ajiboye, T.O., Omotola, E.O., Oyewola, O.J., 2022. Methylene blue dye: Toxicity and potential elimination technology from wastewater. Results in Engineering. https://doi.org/10.1016/j.rineng.2022.100678

Oussalah, A., Boukerroui, A., Aichour, A., Djellouli, B., 2019. Cationic and anionic dyes removal by low-cost hybrid alginate/natural bentonite composite beads: Adsorption and reusability studies. Int J Biol Macromol 124, 854–862. https://doi.org/10.1016/j.ijbiomac.2018.11.197

ACCEPTED MANUSCRIPT

Özcan, A.S., Özcan, A., 2004. Adsorption of acid dyes from aqueous solutions onto acid-activated bentonite. J Colloid Interface Sci 276, 39–46. https://doi.org/10.1016/j.jcis.2004.03.043

Rehman, M.S.U., Kim, I., Han, J.I., 2012. Adsorption of methylene blue dye from aqueous solution by sugar extracted spent rice biomass. Carbohydr Polym 90, 1314–1322. https://doi.org/10.1016/j.carbpol.2012.06.078

Rezende, M.V.S., Pereira, U.C., Rezende, Y.R.R.S., Carvalho, I.S., Silveira, W.S., Junot, D.O., Silva, R.S., Resende, C.X., Ferreira, N.S., 2021. Sustainable preparation of ixora flower-like shaped luminescent powder by recycling crab shell biowaste. Optik (Stuttg) 235. https://doi.org/10.1016/j.ijleo.2021.166636

Ribeiro dos Santos, F., de Oliveira Bruno, H.C., Zelayaran Melgar, L., 2019. Use of bentonite calcined clay as an adsorbent: equilibrium and thermodynamic study of Rhodamine B adsorption in aqueous solution. Environmental Science and Pollution Research 26, 28622–28632. https://doi.org/10.1007/s11356-019-04641-0

Rida, K., Bouraoui, S., Hadnine, S., 2013. Adsorption of methylene blue from aqueous solution by kaolin and zeolite. Appl Clay Sci 83–84, 99–105. https://doi.org/10.1016/j.clay.2013.08.015

Saha, P., Chowdhury, S., Gupta, S., Kumar, I., 2010. Insight into adsorption equilibrium, kinetics and thermodynamics of Malachite Green onto clayey soil of Indian origin. Chemical Engineering Journal 165, 874–882. https://doi.org/10.1016/j.cej.2010.10.048

Şahin, Ö., Kaya, M., Saka, C., 2015. Plasma-surface modification on bentonite clay to improve the performance of adsorption of methylene blue. Appl Clay Sci 116–117, 46–53. https://doi.org/10.1016/j.clay.2015.08.015

Saini, A., Doda, A., Singh, B., 2018. Recent advances in microbial remediation of textile azo dyes, in: Phytobiont and Ecosystem Restitution. Springer Singapore, pp. 45–62. https://doi.org/10.1007/978-981-13-1187-1_3

Samsami, S., Mohamadi, M., Sarrafzadeh, M.H., Rene, E.R., Firoozbahr, M., 2020. Recent advances in the treatment of dye-containing wastewater from textile industries: Overview and perspectives. Process Safety and Environmental Protection. https://doi.org/10.1016/j.psep.2020.05.034

Sankhla, M.S., Kumari, M., Nandan, M., Kumar, R., Agrawal, P., 2016. Heavy Metals Contamination in Water and their Hazardous Effect on Human Health-A Review. Int J Curr Microbiol Appl Sci 5, 759–766. https://doi.org/10.20546/ijcmas.2016.510.082

Shanker, U., Rani, M., Jassal, V., 2017. Degradation of hazardous organic dyes in water by nanomaterials. Environ Chem Lett. https://doi.org/10.1007/s10311-017-0650-2

Sharifi-Bonab, M., Aber, S., Salari, D., Khodam, F., 2020. Synthesis of CoZnAl-layered double hydroxide/graphene oxide nanocomposite for the removal of methylene blue: Kinetic, thermodynamic, and isotherm studies. Environ Prog Sustain Energy 39. https://doi.org/10.1002/ep.13316

Shattar, S.F.A., Zakaria, N.A., Foo, K.Y., 2020. One step acid activation of bentonite derived adsorbent for the effective remediation of the new generation of industrial pesticides. Sci Rep 10, 20151. https://doi.org/10.1038/s41598-020-76723-w

ACCEPTED MANUSCRIPT

Shi, L., Zhang, G., Wei, D., Yan, T., Xue, X., Shi, S., Wei, Q., 2014. Preparation and utilization of anaerobic granular sludge-based biochar for the adsorption of methylene blue from aqueous solutions. J Mol Liq 198, 334–340. https://doi.org/10.1016/j.molliq.2014.07.023

Siddiqui, M.F., Andleeb, S., Ali, N., Ghumro, B., Ahmed, S., 2010. Biotreatment of anthraquinone dye Drimarene Blue K 2 RL, African Journal of Environmental Science and Technology.

Sohrabnezhad, S., Pourahmad, A., 2010. Comparison absorption of new methylene blue dye in zeolite and nanocrystal zeolite. Desalination 256, 84–89. https://doi.org/10.1016/j.desal.2010.02.009

Tkaczyk, A., Mitrowska, K., Posyniak, A., 2020. Synthetic organic dyes as contaminants of the aquatic environment and their implications for ecosystems: A review. Science of the Total Environment. https://doi.org/10.1016/j.scitotenv.2020.137222

Tomar, P.C., Dahiya, P., 2022. Microbial Degradation of Azo Dyes Present in Textile Industry Wastewater, in: Microbial Remediation of Azo Dyes with Prokaryotes. CRC Press, pp. 89–103. https://doi.org/10.1201/9781003130932-7

UNESCO, 2020. UN World Water Development Report 2020 – Water and Climate Change | UNESCO.

Upendar, G., Dutta, S., Bhattacharya, P., Dutta, A., 2017. Bioremediation of methylene blue dye using Bacillus subtilis MTCC 441. Water Science and Technology 75, 1572–1583. https://doi.org/10.2166/wst.2017.031

Wibowo, Y.G., Fauzul Imron, M., Budi Kurniawan, S., Surya Ramadan, B., Taher, T., Hayu Sudibya, A., Syarifuddin, H., Khairurrijal, K., 2023a. Emerging Strategies for Mitigating Acid Mine Drainage Formation and Environmental Impacts: A Comprehensive Review of Recent Advances. Science and Technology Indonesia 8. https://doi.org/10.26554/sti.2023.8.4.516-541

Wibowo, Y.G., Sudibyo, Naswir, M., Ramadan, B.S., 2022. Performance of a novel biochar-clamshell composite for real acid mine drainage treatment. Bioresour Technol Rep 17. https://doi.org/10.1016/j.biteb.2022.100993

Wibowo, Y.G., Syahnur, M.T., Al Azizah, P.S., Aranta, D., Lululangi, B.R., Sudibyo, 2023b. Phytoremediation of High Concentration of Ionic Dyes using Aquatic Plant (Lemna minor): A Potential Eco-Friendly Solution for Wastewater Treatment. Environ Nanotechnol Monit Manag 100849. https://doi.org/10.1016/j.enmm.2023.100849

World Health Organization, 2019. Preventing Disease Through Healthy Environments. Exposure to Arsenic: A Major Public Health Concern.

Yang, D., Cheng, F., Chang, L., Wu, D., 2022. Sodium modification of low quality natural bentonite as enhanced lead ion adsorbent. Colloids Surf A Physicochem Eng Asp 651. https://doi.org/10.1016/j.colsurfa.2022.129753

Yao, X., Ji, L., Guo, J., Ge, S., Lu, W., Cai, L., Wang, Y., Song, W., Zhang, H., 2020. Magnetic activated biochar nanocomposites derived from wakame and its application in methylene blue adsorption. Bioresour Technol 302. https://doi.org/10.1016/j.biortech.2020.122842

Zhang, P., O'Connor, D., Wang, Y., Jiang, L., Xia, T., Wang, L., Tsang, D.C.W., Ok, Y.S., Hou, D., 2020. A green biochar/iron oxide composite for methylene blue removal. J Hazard Mater 384. https://doi.org/10.1016/j.jhazmat.2019.121286

ACCEPTED MANUSCRIPT